

Analytical techniques for addressing forward and inverse problems of light scattering by irregularly shaped particles

Xu Li, Zhigang Chen, Jianmin Gong, Allen Taflove, and Vadim Backman

Department of Biomedical Engineering and Department of Electrical and Computer Engineering,
Northwestern University, Evanston, Illinois 60208

Received December 24, 2003

Understanding light scattering by nonspherical particles is crucial in modeling the transport of light in realistic structures such as biological tissues. We report the application of novel analytical approaches based on modified Wentzel–Kramers–Brillouin and equiphase-sphere methods that facilitate accurate characterization of light scattering by a wide range of irregularly shaped dielectric particles. We also demonstrate that these approaches have the potential to address the inverse-scattering problem by means of a spectral analysis of the total scattering cross section of arbitrarily shaped particles. © 2004 Optical Society of America
OCIS codes: 290.5850, 290.3200, 170.6510.

Most natural particles have nonspherical geometries, and therefore light scattering by irregularly shaped particles is of significant research interest in a variety of disciplines such as astronomy, meteorology, remote sensing, and biomedicine. The development and application of accurate, yet easy to use, inversion-enabling approximations to model light scattering by nonspherical particles is of critical importance. In this Letter we focus our discussion on two such approximate methods, namely, a modified Wentzel–Kramers–Brillouin (WKB) approximation¹ and the recently proposed equiphase sphere (EPS) approximation.² The mathematical simplicity of these methods makes them especially appealing for application to inverse-scattering problems.

Our analysis is focused on the spectral properties of total scattering cross section (TSCS), as the TSCS spectrum is of particular importance in applications such as spectroscopic tissue diagnosis.^{3–6} Previously, the feasibility of applying the modified WKB approximation and the EPS approximation to calculate TSCS spectra of inhomogeneous and spheroidal particles was demonstrated.^{2,7} In this Letter we apply these two methods to predict the orientation-dependent TSCS spectra of particles of arbitrary irregular shapes. We compare the validity and accuracy of these methods and the rigorous numerical solutions to Maxwell's equations, using the finite-difference time-domain⁸ (FDTD) method for a wide range of irregular particles of sizes in the resonance range. We also demonstrate the potential of using these methods to probe the sizes and geometric characteristics of arbitrarily shaped particles from their light-scattering properties.

In both the modified WKB and the EPS approximations the TSCS is given by the sum of two terms, surface effect term $\sigma_s^{(s)}$ and volume scattering term $\sigma_s^{(v)}$. When the high-frequency ripple structure in the TSCS spectrum is neglected (the ripple structure is typically averaged out in realistic experimental measurements), surface term $\sigma_s^{(s)}$ can be approximated as⁷

$$\sigma_s^{(s)} \approx 2S_m(kd/2)^{-2/3}, \quad (1)$$

where S_m is the maximum transverse cross section area, d is the mean diameter, and $k = 2\pi/\lambda$ is the

wave number. In the modified WKB approximation, volume term $\sigma_s^{(v)}$ is given by

$$\sigma_s^{(v)} = 2 \operatorname{Re} \left(\iint_S \{1 - \exp[ik(n-1)L(\mathbf{r})]\} d^2\mathbf{r} \right) \quad (2)$$

for a homogeneous particle. Here, S is the projection area of the particle in the plane transverse to the incident light, \mathbf{r} is a vector in plane S , and $L(\mathbf{r})$ is the path length of the light ray traveling inside the particle through position \mathbf{r} . $L(\mathbf{r})$ is equivalent to the longitudinal extent of the particle corresponding to position \mathbf{r} if one neglects the refraction effect in determining the direction of light propagation.

The EPS approximation simplifies volume term $\sigma_s^{(v)}$ by using an explicit expression²:

$$\sigma_s^{(v)} = 2S[1 - 2n \sin \rho/\rho + 4n \sin^2(\rho/2)/\rho^2], \quad (3)$$

where $\rho = kd(n-1)$ and d is equal to the diameter of the equiphase sphere of the particle. Equation (3) is similar to the approximation given by van de Hulst for a homogeneous spherical particle with a low refractive index and predicts an oscillatory interference structure in the TSCS spectra with a frequency proportional to the particle's size. Previously, Chen *et al.*² demonstrated that TSCSs of spheroids with certain bounds on major-to-minor axis ratios can be approximated by those of their equiphase sphere counterparts with diameters d equal to the spheroids' longitudinal extent. In this Letter we extend the concept of the equiphase sphere to arbitrary particles by choosing d as the longitudinal extent of an ellipsoid that optimally fits the geometry of the particle [with minimum root-mean-square (rms) error].

We use Gaussian random spheres as a test model with which to evaluate the validity and accuracy of both approximate methods. Following the formulation given by Muinonen *et al.*,⁹ the shape of a Gaussian sphere is determined by radial relative standard deviation Δ and by radius-to-angular-distance correlation angle γ . As shown in Figs. 1(a)–1(c), a higher value of Δ results in an increased magnitude of deformation from spheres, whereas, as illustrated

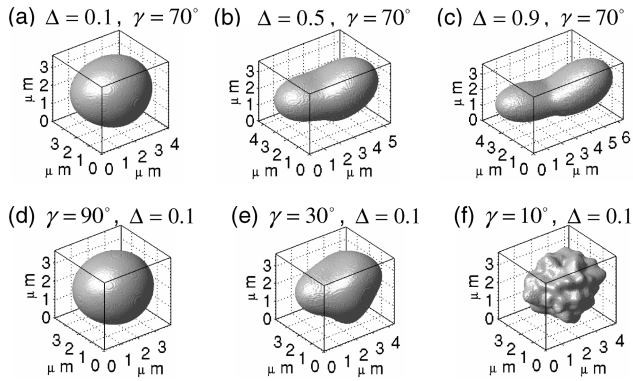


Fig. 1. Representative Gaussian sphere geometries. (a)–(c) Gaussian spheres with increasing Δ (γ is fixed at 70°). (d)–(f) Gaussian spheres with decreasing γ (Δ is fixed at 0.1).

in Figs. 1(d)–1(f), reducing γ leads to increased high-degree terms of the surface perturbation and thus results in increased numbers of valleys and hills on the particle surface. Thus one can represent a wide range of natural and artificial shapes by varying Δ and γ in the Gaussian sphere model.

We used FDTD simulated data as benchmarks to characterize accurately the light-scattering properties of various Gaussian spheres. FDTD simulations were conducted for Gaussian spheres with Δ ranging from 0.1 to 0.9 and γ ranging from 10° to 90° . The particles were assigned a mean diameter of the order of $3.5 \mu\text{m}$ and a refractive index of 1.5. Following the same procedure as described previously,^{3,10} we calculated the frequency-dependent TSCS from the FDTD simulations.

Figure 2 compares TSCS spectra calculated by FDTD simulation by a modified WKB method and by the EPS approximation for four Gaussian spheres with shapes that deviate progressively from that of a sphere. In Figs. 2(a)–2(c) the EPS approximation gives a slightly more accurate estimation of the TSCS than does the modified WKB method. The improved accuracy is due to the fact that the EPS approximation implicitly takes into account the refraction effect for shapes that deviate moderately from spheres or ellipsoids. For the severely deformed particle shown in Fig. 2(d) the oscillatory periodicity of the TSCS spectrum obviously departs from its EPS counterpart. However, the modified WKB approximation still gives a fairly good estimation of the TSCS spectrum.

We used rms error to parameterize the accuracy of the analytical approximations compared with the accurate FDTD data. To investigate the influence of particle irregularity on the approximation accuracy we plotted the rms errors for both approximations as functions of the particle's shape parameters Δ [Fig. 3(a)] and γ [Fig. 3(b)]. As the particles deviate from spherical shapes, the accuracies of both approximations degrade. However, it is evident from Fig. 3 that both methods give TSCS spectra with rms errors of $<5\%$ for a wide range of irregularly shaped particles.

Because of their accuracy demonstrated above, along with their mathematical simplicity, these two approxi-

mate methods have great potential for being applied in inverse-scattering problems for irregularly shaped particles. For the range of shapes at which the EPS approximation is valid, the diameter of the corresponding equiphase sphere d (an estimation of the longitudinal dimension of the particle) can be derived from the oscillation period of the TSCS given by Eq. (3), and, by further fitting the TSCS curve, one can readily find total transverse area S .

We can note from Fig. 3 that the modified WKB approximation has a greater range of validity than the EPS approximation. However, because this method involves numerical integration the inversion procedure is not so straightforward as that provided by the EPS approximation. Here we propose a novel approach to probing the size and shape of a particle from its TSCS spectrum by using the modified WKB approximation, as introduced in the following discussion.

For a homogeneous particle the modified WKB approximation given by approximation (1) and Eq. (2) can be written as

$$\sigma_s = 2S_m(kd/2)^{-2/3} + 2S - 2 \iint_S \cos[k(n-1)L(\mathbf{r})]d^2\mathbf{r}. \quad (4)$$

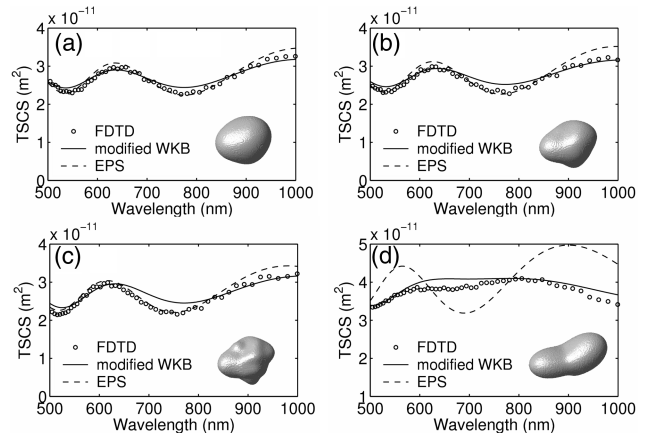


Fig. 2. Comparison of TSCSs calculated from FDTD simulations, the modified WKB approximation, and the EPS approximation for Gaussian spheres with different shapes. The particles are illuminated with vertically directed incident light: (a) $\Delta = 0.1$, $\gamma = 50^\circ$; (b) $\Delta = 0.1$, $\gamma = 30^\circ$; (c) $\Delta = 0.1$, $\gamma = 20^\circ$; (d) $\Delta = 0.7$, $\gamma = 70^\circ$.

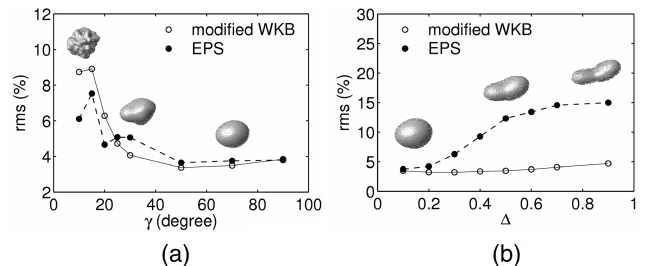


Fig. 3. TSCS spectrum rms error of the modified WKB approximation and the EPS approximation. FDTD simulation results are used as the benchmark data. rms errors (%) as functions of (a) γ (Δ is fixed at 0.1) and (b) Δ (γ is fixed at 70°).

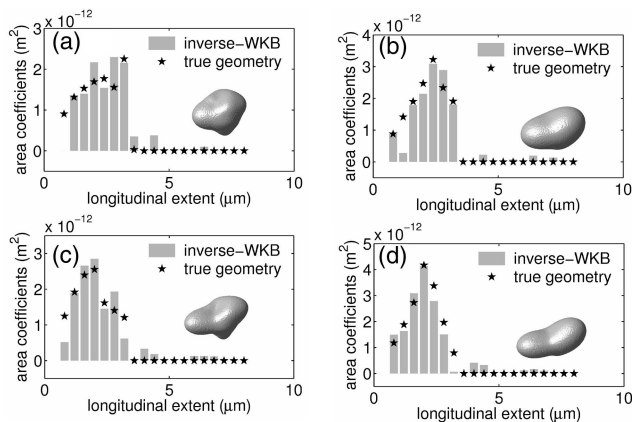


Fig. 4. WKB-reconstructed area distribution of the longitudinal extent, $a_i(L_i)$, for Gaussian spheres with various values of radial relative standard deviations and correlation angles: (a) $\Delta = 0.1$, $\gamma = 25^\circ$; (b) $\Delta = 0.4$, $\gamma = 70^\circ$; (c) $\Delta = 0.2$, $\gamma = 30^\circ$; (d) $\Delta = 0.7$, $\gamma = 70^\circ$.

By dividing the possible range of longitudinal extent $L(\mathbf{r})$ into discrete values L_i we can replace the integration over total transverse area S in Eq. (4) by $\sum_i a_i \cos[k(n-1)L_i]$, where coefficient a_i is the portion of transverse area that corresponds to L_i . Thus, for a given wavelength λ_j , Eq. (4) can be rewritten as

$$\sigma_s(\lambda_j) = \sum_i 2a_i \cos[2\pi(n-1)L_i/\lambda_j] + 2S_m(\pi d)^{-2/3}(\lambda_j)^{2/3} + 2S. \quad (5)$$

If n is known, for a number of preselected values of L_i and wavelengths λ_j a set of linear equations can be formed from Eq. (5) to solve area coefficients a_i and total transverse area S simultaneously.

Because linear equation (5) constitutes an ill-posed problem, one must employ additional *a priori* information to obtain a stable solution. We added two important constraints, i.e., a nonnegativity constraint ($a_i \geq 0$, $S > 0$, $S_m > 0$, and $d > 0$) and an area-consistency constraint ($\sum_i a_i = S \pm \delta$, where δ is a small value chosen empirically) to form a constrained linear least-squares problem that can be solved with an active-set method.¹⁰

Figure 4 plots the area distribution of longitudinal extent reconstructed from TSCS spectra calculated by FDTD simulations for four Gaussian spheres. For all four cases the inversion results are consistent with the true distribution calculated from the original geometry. From these graphs of area coefficients, the volume and the total transverse area of the particles

can easily be derived. Furthermore, the longitudinal-extent distribution profiles are especially useful indicators with which to infer the shape characteristics, such as eccentricity and surface deformation, of particles. For the inversion results presented in this Letter, δ was chosen to be $S/20$. We noted that the robustness of this approach is not sensitive to the choice of δ .

In summary, in this Letter we have introduced novel analytical approaches, based on the modified WKB approximation and the EPS approximation, to the characterization of light scattering by a wide range of irregularly shaped dielectric particles. The discussion in this Letter was focused on light scattering by isolated, nonabsorbing single particles of arbitrary shape and orientation. Improved knowledge of the optical scattering properties of such particles forms the foundation for understanding of light scattering by ensembles of random particles. In turn, this facilitates general advances in the optics of random media, including remote sensing, light propagation in the atmosphere, random-media lasing, and optical tissue diagnosis.

This study was supported in part by National Science Foundation grants BES-0238903 and ACI-0219925. We thank the authors of the original Gaussian-sphere generation code, K. Muinonen and T. Nousiainen, for making the code publicly available. X. Li's e-mail address is xuli@northwestern.edu.

References

1. J. D. Klett and R. A. Sutherland, *Appl. Opt.* **31**, 373 (1992).
2. Z. Chen, A. Taflove, and V. Backman, *J. Opt. Soc. Am. A* **20**, 88 (2004).
3. L. T. Perelman, V. Backman, M. Wallace, G. Zonios, R. Manoharan, A. Nusrat, S. Shields, M. Seiler, C. Lima, T. Hamano, I. Itzkan, J. Van Dam, J. M. Crawford, and M. S. Feld, *Phys. Rev. Lett.* **80**, 627 (1998).
4. A. Wax, C. Yang, and J. A. Izatt, *Opt. Lett.* **28**, 1230 (2003).
5. Y. L. Kim, Y. Liu, R. K. Wali, H. K. Roy, M. J. Goldberg, A. K. Kromine, K. Chen, and V. Backman, *IEEE J. Sel. Top. Quantum Electron.* **9**, 243 (2003).
6. J. R. Mourant, T. M. Johnson, S. Carpenter, A. Guerra, T. Aida, and J. P. Freyer, *J. Biomed. Opt.* **7**, 378 (2002).
7. Z. Chen, A. Taflove, and V. Backman, *Opt. Lett.* **28**, 765 (2003).
8. A. Taflove and S. Hagness, *Computational Electrodynamics: the Finite-Difference Time-Domain Method* (Artech House, Boston, Mass., 2000).
9. K. Muinonen, T. Nousiainen, P. Fast, K. Lumme, and J. I. Peltoniemi, *J. Quant. Spectrosc. Radiat. Transfer* **55**, 577 (1996).
10. P. E. Gill, W. Murray, and M. H. Wright, *Practical Optimization* (Academic, London, 1981).